International Journal of Research in Engineering and Science (IJRES)
ISSN (Online): 2320-9364, ISSN (Print): 2320-9356
www.ijres.org Volume 6 Issue 1 ǁ 1. 2018 ǁ PP. 70-78

Excitation Of Silicon Atom And Singly-Charged Ion In E–Si Collisions

*Smirnov Yu.M.
(Department of Physics-1, National Research University «MPEI», Moscow, Russia)
*Corresponding Author: *Smirnov Yu.M.*

ABSTRACT: Inelastic collisions of low energy electrons with silicon atoms were studied using the method of extended crossing beams with recording of optical signal emitted by excited atoms from the crossing area. Fifty excitation cross-sections of the silicon atom and eight excitation cross-sections of the singly-charged silicon ion have been measured at the incident electron energy of 50 eV. Optical excitation functions (OEFs) have been recorded in the electron energy range of 0–200 eV for transitions originating at three silicon atom levels. The obtained excitation cross-section values have been compared to theoretical results for the silicon atom.

Keywords: silicon atom, excitation cross-section, optical excitation function, energy level, transition, spectral line

Date of Submission: 20-01-2018 Date of acceptance: 08-02-2018

I. INTRODUCTION

The study of physical and chemical properties of the silicon atom is of interest both for fundamental sciences and for numerous technological applications. In terms of cosmic abundance, silicon ranks seventh among the chemical elements. Its emissive lines can be detected both in the solar spectrum and in spectra of Classes B and A stars; its absorption lines are also observed in stars of earlier spectral classes, down to M [1]. Emissive lines of the silicon atom and singly-charged ion have also been discovered over the recent two decades in intensively studied spectra of roAp stars. C, Al, Si, and S are all somewhat underabundant relative to the solar chemical composition, which is typical of roAp stars. An example is provided by HD 213637, a star with silicon content established on the basis of twelve SiI spectral lines and two SiII lines [2].

Silicon finds its technological applications mostly in the field of electronics, quantum electronics included. At the dawn of the laser era, as early as 1965, generation of coherent radiation at transitions of silicon atom was obtained in infrared [3], followed the same year by laser generation using the five transitions of singly-charged and doubly-charged silicon ions in visible [4]. Latter study reported obtaining pulse generation in the positive column of a longitudinal discharge using the sulphur and phosphorus hexafluorides.

Plasma containing silicon atoms and ions may also appear in various process devices. For example, nano-composite Si particle formation by plasma spraying was used in the production process of the negative electrode of Li ion batteries [5]. And besides, high rate amorphous and crystalline silicon formation by pulsed DC magnetron sputtering deposition for photovoltaics was used [6]. Notable examples include also the Czochralski method, widely used for the manufacturing of silicon at electronic-grade purity.
In all these instances plasma appears in a state different from the thermodynamic equilibrium. Information on elementary processes taking place in a plasma is a prerequisite for its diagnostics and computation of its properties. Radiative constants of the silicon atom (oscillator strengths, transition probabilities, radiative lifetimes) have been explored in a vast number of publications – see the bibliography section in the compilation paper [7]. In contrast, there are only one experimental [8] and three theoretical papers [9–11] on the collision cross-section behavior of the silicon atom, while data on excitation of the singly-charged silicon ion is lacking altogether. Fourteen excitation cross-sections of the silicon atom spectral lines, all located within a spectral range of λ = 198–288 nm, were measured with an incident electron energy of 50 eV in [8]. Three optical excitation functions (OEFs) were recorded in the electron energy range of 0–200 eV.

The excitation cross-section for the $^1D_2$ level of the silicon atom excited from the ^3P ground state was computed in a theoretical study [9]. Both the ^3P and $^1D_2$ terms belong to the same $3s^23p^2$ configuration, hence their parities are identical. Both the Hartree-Fock and adiabatic-exchange distorted-wave approximation are used in [9]. Two factors pose significant hindrances to the experimental study of $^1D_2$ level excitation using the method of extended crossing beams: 1. The metastable level $3s^23p^2\ ^1D_2$ of the silicon atom has E = 6298 cm^{-1}

and thus may only give rise to two radiative transitions $3s^2 3p^2\ ^3P_{1,2} - 3s^2 3p^2\ ^1D_2$ not forbidden by ΔJ selection rules. At the same time both transitions are forbidden strongly in terms of multiplicity and especially in terms of parity. The $^1D_2$ level result to be rather long-living as a consequence of these exclusion conditions, causing a significant fraction of excited atoms to lose their excitation energy not by spontaneous emission but rather as a result of non-radiative collisions with vacuum chamber walls. A similar situation was studied in detail in the case of the bismuth atom [12]. 2. Owing to a rather small excitation energy of the $^1D_2$ level both ΔJ-allowed radiative transitions from there lie around $\lambda = 1.6$ μm in the IR part of the spectrum. Emission receivers are much less sensitive in this range than are visible-light receivers. Moreover, background glow – a persistent feature of any setup – becomes especially pronounced at $\lambda > 1$ μm.

A later theoretical paper [10] shows excitation cross-sections computed using the Born approximation for fourteen SiI spectral lines within the wavelength range $\lambda = 243–410$ nm. An intermediate coupling scheme for atomic wave functions was used in the computation. Radial wave functions were determined using a semi-empirical method. Cross-section values at incident electron energies $E = 50$, 100, 200 eV were calculated in accordance with the Bethe formula. Thermal population of ground term levels in accordance with the Boltzmann distribution law was taken into account to ensure that theoretical findings can be validly compared with experimental data.

For the most intense SiI spectral lines the discrepancy between theoretical [10] and experimental [8] studies in terms of absolute cross-section values at incident electron energy of $E = 50$ eV was greater than one decimal order. Overall, findings in [8] should be treated as tentative, as they were obtained at an early stage of experimentation with extended crossing beams when substantial refinement was still in order for the experimental technology and method. In particular, measurements of the mass of atom film deposed as absolute cross-section values are scaled have become much more precise by now. Atom concentrations in the beam can now be determined with improved precision as a result. Moreover, molecular nitrogen bands that served as an emission intensity reference prior to 1983 have been replaced with spectral lines of the helium atom [13]. A range of new systems and units have been designed, including an atom beam concentration stabilization system, the non-linear energy sweep unit with a unit to divide photocurrent by electron beam current for OEF recording, a safety circuit protecting the low-voltage electron gun against interelectrode breakdown etc. This work on modernization of apparatus and method had been mostly completed by 1983.

To determine a scale of cross-section absolute values, use should be made of an addition radiation source chosen as an intensity standard. Thereby, to make this change properly, a very important point is to ensure that there are not great differences in the shapes and sizes of the investigated radiator and the standard one. Not considering the geometry factors may be a source a rather significant experimental error. In this experiment neither of the existing standard sources of radiation is a correct change of the extended radiating volume. Therefore, as an intensity standard (exactly speaking, a cross-section standard) the radiation of helium atoms was used; the latter was flowed into the collision space instead of the investigated atoms in the course of the calibration experiments and excited under the same conditions as the atoms of interest.

The choice of helium was dictated by the following reasons: (1) Helium content in the atmosphere and in the residual gases of the vacuum system is negligible. (2) Helium is chemically inert enough. (3) The helium spectrum consists of a relatively small number of lines that are distributed conveniently over wavelengths and intensities. (4) In the work [13], the excitation cross-sections for four spectral lines of helium atom are measured with the highest obtained accuracy. Values of the HeI excitation cross-sections are determined in [13] at 50 and 100 eV electron energies with experimental errors of 9 and 7%, respectively.

In calibration measurements the intensity of the helium lines that are chosen as standards as well as the intensity of one of the spectral lines of an element investigated, are recorded. During the whole experiment a stable regime of evaporation is maintained and controlled by means of continuous recording of the standard line intensity on a diagram. The concentration of helium atoms is determined by an ionization gauge that is calibrated against helium at the calibration plant using a McLeod gauge. The atom concentration of the element under investigation is determined from the mass of a thin film that condenses for a definite time on eight calibration plates of titanium foil placed on a removable grid. The film mass on each plate is about 1 mg and measured with an accuracy of 0.01 mg. Since, as a result of physical and chemical sorption, the film depth may include molecules of residual gases, the film composition is determined by the method of X-ray electron spectroscopy (ESCA). Measurements are carried out of the surface layer composition and then, after etching the latter with a beam of argon ions, the layer composition in the film depth is investigated. On the basis of ESCA results a correction is applied to the scale of cross-section absolute values.

Only recently has a theoretical study [11] been published wherein the *B*-spline *R*-matrix method is used. Both correlation and polarization effects are found to be important for accurate calculations of the cross-sections. Even though the electron shell of the silicon atom cannot be said to be particularly complex, [11] cites great difficulties to computational accuracy: "Neutral silicon can be considered a strongly correlated four-electron system in the $1s^2 2s^2 2p^6$ core potential. This makes it very difficult to obtain accurate wave functions by standard Hartree-Fock (HF) or multiconfiguration Hartree-Fock (MCHF) methods. As shown in recent large-scale MCHF calculations of oscillator strengths in Si [14], well-converged results were only achieved with very extensive expansions containing up to 20000 configurations" [11, P. 022711-1]. And further: "Since the *B*-spline bound-state close-coupling calculations different nonorthogonal sets of orbitals for each atomic state, their subsequent use is somewhat complicated. On the other hand, our configuration expansions for the atomic target states contained at most 200 configurations for each state and hence could be used in the collision calculations with moderate computational resources" [11, P. 022711-2]. Cross-sections have been determined in [11] for excitation both from the ground state $3s^2 3p^2\ ^3P$ and from low-lying metastable levels, $3s^2 3p^2\ ^1D_2$ and $3s^2 3p^2\ ^1S_0$. The two latter cases have not been explored in our experiments while our experimental findings for excitation from the $3s^2 3p^2\ ^3P$ ground term levels can be compared with findings from [10, 11].

However not a single experimental study of excitation cross-sections of the silicon atom and its singly-charged ion has been published since 1981. Thus it was the objective of present study to apply the advanced method of extended crossing beams for examination of SiI and SiII excitation in silicon atom collisions with electrons. Recent publications [15, 16] have already provided detailed treatment of the state-of-the art implementation of this method, therefore it would be superfluous to give a detailed account of the experimental technique and method here. We will only note that despite silicon atom concentration in the beam being as low as $n = 2.3 \times 10^9$ cm^{-3} (almost six times less than in [8]), the present findings are both extensive and more reliable.

The value n indicated above was obtained at evaporation temperature $T = 1800$ K. The J-split of the silicon atom ground term $3s^2 3p^2\ ^3P_J$ is rather modest; the level $3s^2 3p^2\ ^3P_1$ is away from the ground level $3s^2 3p^2\ ^3P_0$ by an energy interval $\Delta E = 77.11$ cm^{-1} while the level $3s^2 3p^2\ ^3P_2$ has $\Delta E = 223.16$ cm^{-1}. For that reason evaporation of silicon atoms at the temperature indicated above takes place simultaneously with thermal population of $J = 1$, 2 levels at the expense of the $J = 0$ level (the ground level). Assuming that the Boltzmann distribution law holds, level populations may be estimated as follows (as percentages of the total atom concentration in the beam): for the level $3s^2 3p^2\ ^3P_0$, $n = 12.5$; for $3s^2 3p^2\ ^3P_1$, $n = 35.3$; for $3s^2 3p^2\ ^3P_2$, $n = 52.2$. Thus, more than half of atoms stay at the highest-lying level of the ground term prior to their collision with electrons. The closest excited level $3s^2 3p^2\ ^1D_2$ (a metastable level $E = 6298$ cm^{-1}) has a population of 0.4%. The distribution of atoms across low-lying levels is taken into account in [10] and in a number of other Peterkop's papers for the sake of more correct comparison between theoretical cross-section values and experimental ones.

For the most intense SiI lines occurring within a spectral range of $\lambda = 250$–253 nm, Q_{50} values have been measured with relative error of ±(3–5)%, the error range for the remaining lines is ±(8–18)% depending on intensity of the each line and its position within the spectrum. The corresponding absolute error range is ±(15–17)% for the most intense lines and ±(20–30)% for all others. Optical excitation functions were recorded in the analog mode, with each plotted as an average over 3 instances. No instance deviated from the average value by more than 7%.

II. RESULTS AND DISCUSSION

The optical spectrum resulting from the bombardment of silicon atoms with electrons of 50 eV energy has been recorded within a spectral range $\lambda = 197$–600 nm. Three optical excitation functions (OEFs) have been recorded with the exciting electron energy varying between 0 eV and 200 eV. All three OEFs correspond to transitions from low-lying excited levels $3s^2 3p4s\ ^3P°_J$ to the ground term levels $3s^2 3p^2\ ^3P_J$ as well as singlet levels $3s^2 3p^2\ ^1S_0$ and $3s^2 3p^2\ ^1D_2$. OEFs could not be recorded reliably enough for transitions originating from higher-lying levels as their absolute excitation cross-sections turned out to be much less than for transitions from $3s^2 3p4s\ ^3P°_J$ levels.

Table 1 summarizes findings for transitions with recorded OEFs. It indicates wavelengths λ, transitions, quantum numbers of the total electron shell moment for the lower J_{low} and upper J_{up} levels, energies of the lower E_{low} and upper E_{up} levels, excitation cross-sections at exciting electron energy of 50 eV Q_{50} and at OEF maximum Q_{max}, and the position of the maximum $E(Q_{\text{max}})$. The last column indicates OEF curve numbers in

accordance with their numbering in Fig. 1. Fig. 1 follows the conventional format for representing atomic OEFs: logarithmic horizontal scale and linear vertical scale with individual zero positions for each curve. Shift of zero positions permit to prevent curves from intersecting or overlapping. Each OEF is normalized to unity at its maximum. Similar data on SiI transitions for which OEFs could not be recorded sufficiently reliably are provided in Table 2, which differs from Table 1 by having its last three columns omitted. Furthermore, Table 2 provides eight Q_{50} cross-section values for transitions of the singly-charged ion; a blend occurs here in a single instance. Almost all measured cross-sections for SiII apparently belong to $3s^2 3d\ ^2D_J – 3s^2 nf\ ^2F°_{J'}$ transitions from n = 4, 5, 6, 7, the only exception being the $3s^2 5s\ ^2S_{1/2} – 3s3p4s\ ^2P°_{3/2}$ transition.

Table 1 Excitation Cross-Sections of Silicon Atom (with OEFs recorded)

□ (nm)	Transition	$J_{low}–J_{up}$	E_{low} (cm^{-1})	E_{up} (cm^{-1})	Q_{50} (10^{-18} cm^2)	Q_{max} (10^{-18} cm^2)	$E(Q_{max})$ (eV)	OEF
250.690	$3s^2 3p^2\ ^3P – 3s^2 3p4s\ ^3P$□	1–2	77	39955	10.3	15.8	11.3	3
251.432	$3s^2 3p^2\ ^3P – 3s^2 3p4s\ ^3P$□	0–1	0	39760	9.22	14.3	11.0	2
251.611	$3s^2 3p^2\ ^3P – 3s^2 3p4s\ ^3P$□	2–2	223	39955	31.1	46.0	11.3	3
251.920	$3s^2 3p^2\ ^3P – 3s^2 3p4s\ ^3P$□	1–1	77	39760	6.96	10.8	11.0	2
252.411	$3s^2 3p^2\ ^3P – 3s^2 3p4s\ ^3P$□	1–0	77	39683	9.53	12.4	10.0	1
252.851	$3s^2 3p^2\ ^3P – 3s^2 3p4s\ ^3P$□	2–1	223	39760	12.4	19.2	11.0	2
297.035	$3s^2 3p^2\ ^1D – 3s^2 3p4s\ ^3P$□	2–2	6298	39955	0.66	1.01	11.3	3
298.765	$3s^2 3p^2\ ^1D – 3s^2 3p4s\ ^3P$□	2–1	6298	39760	0.57	0.88	11.0	2
410.294	$3s^2 3p^2\ ^1S – 3s^2 3p4s\ ^3P$□	0–1	15394	39760	0.72	1.12	11.0	2

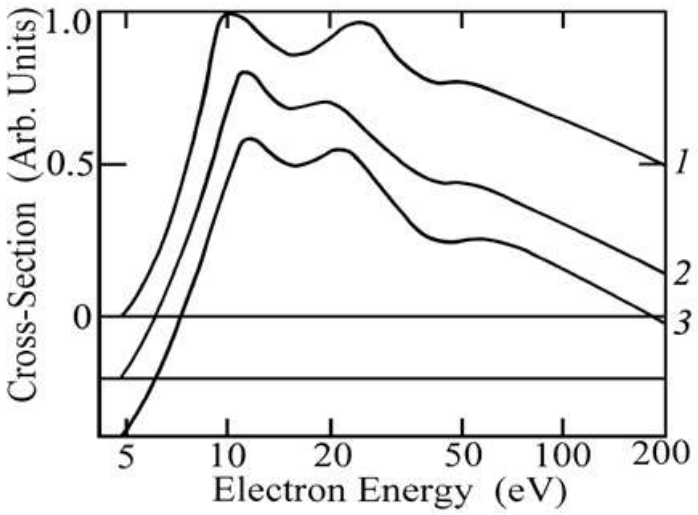

Fig. 1 Optical excitation functions of silicon atom

Reference spectroscopic properties of SiI and SiII are cited from the compilation [17]. The LS coupling notation is used for the classification of low-lying (E < 58770 cm -1) as well as several higher-lying SiI levels. The configuration composition was only computed for odd levels. The role of configuration mixing is relatively modest: only for 3s3p 3 3D°J levels does admixture with 3pnd 3D° reach 39% as it remains below 27% for the rest of odd levels. Most levels lying above E = 58774 cm -1 are assigned on the basis of J1j coupling; they also feature remarkable purity with primary component content never dropping below 50% for all levels having E < 64300 cm -1 .

In the case of the singly-charged silicon ion, component fractions have only been quantified for 14 even and odd levels with E < 103600 cm-1 as well as 18 even levels belonging to the 3s3p(3P°)4f configuration that lie within the energy range 155570 < E < 157490 cm-1 (all energies are counted from the ion ground state). For all SiII levels studied, configuration mixing is just as modest as in the case of SiI. It can thus be assumed that excitation cross-sections can be computed satisfactorily using the Born approximation without accounting for

configuration mixing.

Fig. 2 shows a state diagram for the silicon atom with transitions investigated in this study. Vertical dashed lines are used as dividers for states with different parities. State parameters were removed from the plot area and placed under the horizontal axis as far as possible. When multiple terms correspond to a single Excitationof Silicon Atomand Singly-Charged Ion in e–SiCollisions www.ijres.org 74 | Page configuration, their respective labels are indicated in the plot area. Also values of n are indicated in large type within the plot area. Due to negligible J-split of triplet and quintet terms they are shown without the split, with the exception of 3s 2 3p 2 3P ground term. As its split is rather narrow (ΔE = 223 cm-1) it is shown not to scale. J values

Table 2 Excitation Cross-Sections of Silicon Atom (without OEFs recorded) and Singly-Charged Ion

λ (nm)	Transition	J_{low}–J_{up}	E_{low} (cm^{-1})	E_{up} (cm^{-1})	Q_{50} (10^{-18} cm^2)
1	2	3	4	5	6
I 197.760	$3s^2 3p^2\ ^3P$–$3s^2 3p3d\ ^3P^\circ$	0–1	0	50566	0.35
197.921	$3s^2 3p^2\ ^3P$–$3s^2 3p3d\ ^3P^\circ$	1–0	77	50602	0.71
198.062	$3s^2 3p^2\ ^3P$–$3s^2 3p3d\ ^3P^\circ$	1–1	77	50566	0.68
198.323	$3s^2 3p^2\ ^3P$–$3s^2 3p3d\ ^3P^\circ$	1–2	77	50499	0.46
198.443	$3s^2 3p^2\ ^1D$–$3s^2 3p4d\ ^3P^\circ$	2–2	6298	56690	0.17
198.636	$3s^2 3p^2\ ^3P$–$3s^2 3p3d\ ^3P^\circ$	2–1	223	50566	0.21
198.899	$3s^2 3p^2\ ^3P$–$3s^2 3p3d\ ^3P^\circ$	2–2	223	50499	0.94
199.185	$3s^2 3p^2\ ^1D$–$3s^2 3p4d\ ^1D^\circ$	2–2	6298	56503	1.16
201.097	$3s^2 3p^2\ ^3P$–$3s^2 3p3d\ ^3F^\circ$	2–3	223	49933	0.51
205.483	$3s3p^3\ ^5S^\circ$–$3s3p^2 4s\ ^5P$	2–3	33326	81976	0.29
206.119	$3s3p^3\ ^5S^\circ$–$3s3p^2 4s\ ^5P$	2–2	33326	81826	0.22
206.552	$3s3p^3\ ^5S^\circ$–$3s3p^2 4s\ ^5P$	2–1	33326	81724	0.17
208.447	$3s^2 3p^2\ ^1D$–$3s^2 3p3d\ ^3D^\circ$	2–3	6298	54257	0.42
209.421	$3s^2 3p^2\ ^1S$–$3s^2 3p8s$ (3/2,1/2)°	0–1	15394	63130	0.11
211.463	$3s^2 3p^2\ ^3P$–$3s^2 3p3d\ ^1D^\circ$	1–2	77	47351	0.96
212.119	$3s^2 3p^2\ ^3P$–$3s^2 3p3d\ ^1D^\circ$	2–2	223	47351	0.17
212.299	$3s^2 3p^2\ ^1D$–$3s^2 3p3d\ ^1P^\circ$	2–1	6298	53387	0.53
212.412	$3s^2 3p^2\ ^1D$–$3s^2 3p3d\ ^1F^\circ$	2–3	6298	53362	1.79
220.798	$3s^2 3p^2\ ^3P$–$3s3p^3\ ^3D^\circ$	0–1	0	45276	2.16
221.089	$3s^2 3p^2\ ^3P$–$3s3p^3\ ^3D^\circ$	1–2	77	45293	6.57
221.174	$3s^2 3p^2\ ^3P$–$3s3p^3\ ^3D^\circ$	1–1	77	45276	3.59
221.667	$3s^2 3p^2\ ^3P$–$3s3p^3\ ^3D^\circ$	2–3	223	45321	9.68
221.806	$3s^2 3p^2\ ^3P$–$3s3p^3\ ^3D^\circ$	2–2	223	45293	5.12
221.891	$3s^2 3p^2\ ^3P$–$3s3p^3\ ^3D^\circ$	2–1	223	45276	1.71
228.961	$3s^2 3p^2\ ^1S$–$3s^2 3p4d\ ^3D^\circ$	0–1	15394	59056	0.28
229.103	$3s^2 3p^2\ ^1D$–$3s^2 3p3d\ ^3F^\circ$	2–3	6298	49933	0.65
1	2	3	4	5	6
243.515	$3s^2 3p^2\ ^1D$–$3s^2 3p3d\ ^1D^\circ$	2–2	6298	47351	1.83
243.877	$3s^2 3p^2\ ^3P$–$3s^2 3p4s\ ^1P^\circ$	0–1	0	40991	0.11
244.336	$3s^2 3p^2\ ^3P$–$3s^2 3p4s\ ^1P^\circ$	1–1	77	40991	0.27
245.212	$3s^2 3p^2\ ^3P$–$3s^2 3p4s\ ^1P^\circ$	2–1	223	40991	0.33
253.238	$3s^2 3p^2\ ^1S$–$3s^2 3p5s\ ^1P^\circ$	0–1	15394	54871	1.15
256.864	$3s^2 3p^2\ ^1S$–$3s^2 3p5s\ ^3P^\circ$	0–1	15394	54313	0.51
257.715	$3s^2 3p^2\ ^1S$–$3s^2 3p3d\ ^3D^\circ$	0–1	15394	54185	0.34
263.128	$3s^2 3p^2\ ^1S$–$3s^2 3p3d\ ^1P^\circ$	0–1	15394	53387	0.87
288.158	$3s^2 3p^2\ ^1D$–$3s^2 3p4s\ ^1P^\circ$	2–1	6298	40991	1.83
390.553	$3s^2 3p^2\ ^1S$–$3s^2 3p4s\ ^1P^\circ$	0–1	15394	40991	0.29
475.528	$3s^2 3p4s\ ^3P^\circ$–$3s^2 3p6p$ (3/2,3/2)	0–1	39683	60706	0.25
478.299	$3s^2 3p4s\ ^3P^\circ$–$3s^2 3p6p$ (3/2,1/2)	2–1	39955	60856	0.33
482.117	$3s^2 3p4s\ ^3P^\circ$–$3s^2 3p6p$ (1/2,3/2)	1–2	39760	60496	0.21
551.753	$3s^2 3p4s\ ^1P^\circ$–$3s^2 3p4f\ ^2$[5/2]	1–2	40991	59110	0.54
II 250.093	$3s^2 3d\ ^2D$–$3s^2 6f\ ^2F^\circ$	3/2–5/2	79338	119311	0.28
250.197	$3s^2 3d\ ^2D$–$3s^2 6f\ ^2F^\circ$	5/2–7/2	79355	119311	0.45

290.428	$3s^2 3d\,^2D–3s^2 5f\,^2F°$	3/2–5/2	79338	113760	0.38
290.569	$3s^2 3d\,^2D–3s^2 5f\,^2F°$	5/2–7/2	79355	113760	0.59
412.805	$3s^2 3d\,^2D–3s^2 4f\,^2F°$	3/2–5/2	79338	103556	0.51
413.089	$3s^2 3d\,^2D–3s^2 4f\,^2F°$	5/2–7/2	79355	103556	0.85
423.286	$3s^2 5s\,^2S–3s3p4s\,^2P°$	1/2–3/2	97972	121590	0.77
462.142	$3s^2 4d\,^2D–3s^2 7f\,^2F°$	3/2–5/2	101023	122655	} 0.36
462.172	$3s^2 4d\,^2D–3s^2 7f\,^2F°$	5/2–7/2	101024	122655	

In the case of the singly-charged silicon ion, component fractions have only been quantified for 14 even and odd levels with $E < 103600$ cm^{-1} as well as 18 even levels belonging to the $3s3p(\,^3P°)4f$ configuration that lie within the energy range $155570 < E < 157490$ cm^{-1} (all energies are counted from the ion ground state). For all SiII levels studied, configuration mixing is just as modest as in the case of SiI. It can thus be assumed that excitation cross-sections can be computed satisfactorily using the Born approximation without accounting for configuration mixing.

Fig. 2 shows a state diagram for the silicon atom with transitions investigated in this study. Vertical dashed lines are used as dividers for states with different parities. State parameters were removed from the plot area and placed under the horizontal axis as far as possible. When multiple terms correspond to a single configuration, their respective labels are indicated in the plot area. Also values of n are indicated in large type within the plot area. Due to negligible J-split of triplet and quintet terms they are shown without the split, with the exception of $3s^2 3p^2\,^3P$ ground term. As its split is rather narrow ($\Delta E = 223$ cm^{-1}) it is shown not to scale. J values are indicated to the right of levels in this case.

It can be seen in Fig. 2 that the majority of transitions studied terminate at even terms belonging to the $3s^2 3p^2$ configuration. Besides the $3s^2 3p^2\,^3P$ ground term these also include $3s^2 3p^2\,^1S$ and $3s^2 3p^2\,^1D$ singlet terms. Furthermore, transitions from even levels of the $3s^2 3p(^3P°)6p$ configuration nominated in the J_1j-coupling notation to levels of the $3s^2 3p4s\,^3P°_J$ triplet term have been recorded. Holding an isolated position are the three transitions studied in the quintet term system $3s3p^3\,^5S°_2–3s3p^2(^4P)4s\,^5P_J$.

As mentioned in the Introduction, laser generation based on transitions of singly-charged silicon ions was obtained as early as in 1965 [4]. However all three generation lines λ = 634.710, 637.136, 667.188 nm lie beyond the spectral range investigated by us. They originate from somewhat high-lying upper levels $3s^2(^1S)4p\,^2P°_{1/2,3/2}$ ($E \sim 81200$ cm^{-1}, the first two of the lines mentioned above) and an even higher-lying level $3s3p(^3P°)4p\,^4D_{7/2}$ ($E = 132162$ cm^{-1}). These energies have been counted also from the ground level of the singly-charged ion. When these levels are excited by electron impact from the ground state of the atom, i.e. by excitation with simultaneous single ionization, their excitation cross-sections would be presumably rather small.

Excitation cross-section values obtained in this experiment for the silicon atom can be compared with theoretical values computed using the Born approximation [10]. This comparison is presented in Table 3 which is supplemented with computed Q_{50} values from [10] and Q[P.p.]/Q[10] ratios in addition to the cross-section values containing in preceding tables. It can be seen in the last column, all cross-sections listed in Table 3 fall into three groups: 1. The six most intense lines feature entirely allowed transitions $3s^2 3p^2\,^3P–3s^2 3p4s\,^3P°$ having $Q_{50} > 7.8 \times 10^{-18}$ cm^2. The corresponding average value is $(Q\text{[P.p.]}/Q\text{[10]})_{aver} = 0.88 \pm 0.06$. 2. Three medium-intensity transitions with two occurring within the singlet term system and the third being an intercombination one. The corresponding cross-section values are $(0.15 \le Q_{50} \le 1.00) \times 10^{-18}$ cm^2. These transitions have $1.36 < Q\text{[P.p.]}/Q\text{[10]} < 1.93$, with the mean ratio being 1.71. 3. Five lines of the least intensity having $Q_{50} \le 0.054 \times 10^{-18}$ cm^2. Experimental cross-section values for these transitions exceed their theoretical counterparts essentially: $(Q\text{[P.p.]}/Q\text{[10]})_{aver} = 28.6$ with a great dispersion.

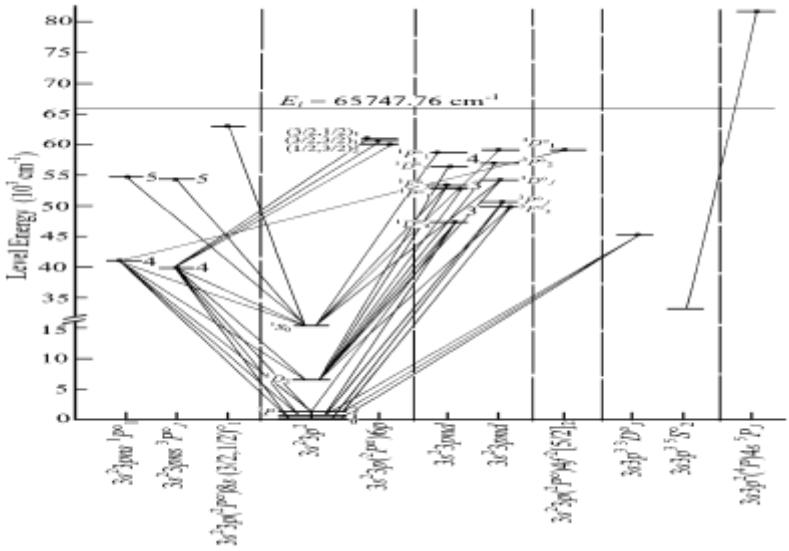

Fig. 2 Partial state diagram of SiI.

Table 3 Comparison of experimental *Q*[P.p.] and theoretical *Q*[10] absolute cross-sections

λ (nm)	Transition	J_{low} –J_{up}	E_{low} (cm^{-1})	E_{up} (cm^{-1})	Q_{50} (10^{-18} cm^2) [P.p.]	Q_{50} (10^{-18} cm^2) [10]	*Q*[P.p.]/*Q*[10]
243.877	$3s^23p^2\,^3P–3s^23p4s\,^1P°$	0–1	0	40991	0.11	0.0020	55.
244.336	$3s^23p^2\,^3P–3s^23p4s\,^1P°$	1–1	77	40991	0.27	0.019	14.2
245.212	$3s^23p^2\,^3P–3s^23p4s\,^1P°$	2–1	223	40991	0.33	0.013	25.4
250.690	$3s^23p^2\,^3P–3s^23p4s\,^3P°$	1–2	77	39955	10.3	12.2	0.85
251.432	$3s^23p^2\,^3P–3s^23p4s\,^3P°$	0–1	0	39760	9.22	10.5	0.88
251.611	$3s^23p^2\,^3P–3s^23p4s\,^3P°$	2–2	223	39955	31.1	36.4	0.86
251.920	$3s^23p^2\,^3P–3s^23p4s\,^3P°$	1–1	77	39760	6.96	7.8	0.89
252.411	$3s^23p^2\,^3P–3s^23p4s\,^3P°$	1–0	77	39683	9.53	11.1	0.86
252.851	$3s^23p^2\,^3P–3s^23p4s\,^3P°$	2–1	223	39760	12.4	13.2	0.94
288.158	$3s^23p^2\,^1D–3s^23p4s\,^1P°$	2–1	6298	40991	1.83	1.0	1.83
297.035	$3s^23p^2\,^1D–3s^23p4s\,^3P°$	2–2	6298	39955	0.66	0.019	34.7
298.765	$3s^23p^2\,^1D–3s^23p4s\,^3P°$	2–1	6298	39760	0.57	0.42	1.36
390.553	$3s^23p^2\,^1S–3s^23p4s\,^1P°$	0–1	15394	40991	0.29	0.15	1.93
410.294	$3s^23p^2\,^1S–3s^23p4s\,^3P°$	0–1	15394	39760	0.72	0.054	13.6

A comparison with recent computational findings from [11] is only possible for excitation cross-sections of terms as computations in [11] have been performed without accounting for *J*-split of terms. As indicated in the Introduction, cross-sections are fit for comparison of levels only excited from the ground term ^3P. However we have been unable to study the $^3P\rightarrow\,^1S$ and $^3P\rightarrow\,^1D$ excitations; transitions associated with excitation of $3s^23p4p\,^3P$ even levels have similarly remained undetected by us. Our experimental setup permit us to identify excitation of only $3s3p^24p\,^5P$ and $3s^23p4f\,^2[5/2]_2$ even levels. Furthermore, in $3s^23p4s\,^3P°–3s^23p6p\,^2[J_1,j]$ transitions participate three high-lying even levels of the $3s^23p6p$ configuration that belong to three distinct terms in the J_1j-coupling notation.

This leaves us with just three excitation processes for which excitation cross-sections can be compared: $3s^23p^2\,^3P–3s^23p4s\,^3P°$, $3s^23p^2\,^3P–3s3p^3\,^3D°$, $3s^23p^2\,^3P–3s^23p3d\,^3D°$. Excitation cross-section values are not tabulated in [11]. They are only plotted on small-scale charts. If Q_{50} values were read directly from the charts [11, Fig. 2] they would be as follows: 96×10^{-18} cm^2 for $3s^23p4s\,^3P°$; 20×10^{-18} cm^2 for $3s3p^3\,^3D°$; 56×10^{-18} cm^2 for $3s^23p3d\,^3D°$. Our experimental findings for transitions from the corresponding term obtained by summation of cross-sections over *J* are: 81.5×10^{-18} cm^2 for $3s^23p4s\,^3P°$; 28.8×10^{-18} cm^2 for $3s3p^3\,^3D°$. For $3s^23p3d\,^3D°$ the 0.76×10^{-18} cm^2 reading has been obtained by addition together cross-sections for the least intense (intercombination) transitions whereas the remaining, significantly more intense transitions from $3s^23p3d\,^3D°$ to the ground term levels all lie in the vacuum UV part of the spectrum at λ ~ 185 nm, beyond the

reach of our instruments. Thus it follows from the reported data that experimental cross-section values for $3s^2 3p4s\ ^3P°$ levels are 15% smaller than the respective theoretical values proposed in [11] while being 30% greater for $3s3p^3\ ^3D°$ levels. It should be noted that the theoretical computation of cross-sections in [11] only accounts for the direct electron-impact excitation of the upper levels in question from the ground state. In contrast, the experiment achieves population of the same upper levels both by direct excitation and as a result of cascade population caused by spontaneous transitions from higher-lying levels.

In present study majority of transitions from the high-lying levels terminate at metastable levels E = 6298, 15394, 33326 cm^{-1} or at levels of the ground term. The longest-wavelength of the recorded transitions, λ = 551.753 nm, takes part in the cascade population of the $3s^2 3p4s\ ^1P°_1$ E = 40991 cm^{-1} singlet level. Only three transitions from levels that belong to the $3s^2 3p6p$ configuration are involved in the population of the $3s^2 3p4s\ ^3P°$ term. Their total cross-section is $\Sigma Q_{50} = 0.79 \times 10^{-18}$ cm^2 – less than 1% of the complete $3s^2 3p4s\ ^3P°$ term excitation cross-section $\Sigma Q_{50} = 81.5 \times 10^{-18}$ cm^2. The somewhat more intense transitions to levels of the same term within λ = 570–590 nm have not been detected by us due to increased noise as photoreceiver sensitivity falls off sharply and background glow increases appreciably when approaching λ = 600 nm.

III. SUMMARY

Excitation of spectral lines of the silicon atom and singly-charged ion in collisions of silicon atoms with slow electrons has been studied in detail. For SiI most intense spectral lines measured excitation cross-sections were on the average 0.88 times of the theoretical estimates computed using the Born approximation. The excitation cross-section of the $3s^2 3p4s\ ^3P°$ term is 15% smaller than the theoretical value obtained using the *B*-spline *R*-matrix method [11]. Thus, experimental cross-section readings are in a good agreement with findings from theoretical studies [10, 11]. The resulting information can be useful for computational simulation of low-temperature plasma lasers and process units containing silicon vapor as well as for non-LTE astrophysics problems.

REFERENCES

[1]. Merrill P W, Lines of the chemical elements in astronomical spectra (Washington, Carnegie Inst. of Washington publ., 1956)

[2]. Kochukov O, Atmospheric parameters and chemical composition of the ultra-cool roAp star HD 213637*, Astron. Astrophys., 404 (4), 2003, 669–676.

[3]. Shimazu M and Suzaki Y, Laser oscillation in silicon tetrachloride vapor, Japan. J. Appl. Phys., 4 (10)**,** 1965, 819.

[4]. Cheo P K and Cooper G H, UV and visible laser oscillations in fluorine, phosphorus and chlorine, Appl. Phys. Lett., 7 (7), 1965, 202–204.

[5]. Kambara M, Kitayama A, Homma K, et al., Nano-composite Si particle for formation by plasma spraying for negative electrode of Li ion batteries, J. Appl. Phys., 115 (14)**,** 2014, 143302.

[6]. Bailey L R, Proudfoot G, Mackenzie B, et al., High rate amorphous and crystalline silicon formation by pulsed DC magnetron sputtering deposition for photovoltaics was used, Phys. status solidi A, 212 (1), 2015, 42–46.

[7]. Kelleher D E and Podobedova L I, Atomic transition probabilities of silicon. A critical compilation, J. Phys. Chem. Ref. Data, 37 (6)**,** 2008, 1285–1501.

[8]. Kolosov P A, Krasavin A Yu and Smirnov Yu M, Excitation cross-sections of silicon atom by electron impact, Astronomicheskiy Jurnal (in Rus., Astronomy Reports) 58 (6), 1981, 1213–1216.

[9]. Pindzola M S, Bhatia A K and Temkin A, Electron impact excitation of carbon and silicon in the distorted-wave approximation, Phys. Rev. A, 15 (1), 1977, 35–42.

[10]. Peterkop R K, Calculation of excitation cross-sections and oscillator strengths of the silicon and germanium atoms, Optika i Spektroskopiya (in Rus., Optics and Spectroscopy), 58 (1), 1985, 202–204.

[11]. Gedeon V, Gedeon S, Lazur V, et al., Electron scattering from silicon, Phys. Rev. A, 85, 2012, 022711 (7pp.).

[12]. Smirnov Yu M, Excitation of the bismuth forbidden transitions by electron impact, Jurnal Technicheskoy Fiziki (Pisma) (in Rus., Journal of the Technical Physics, Letters), 11 (11), 1985, 689–693.

[13]. Van Zyl B, Dunn G H, Chamberlain G and Heddle D W O, Benchmark cross-sections for electron-impact excitation of helium atom, Phys. Rev. A, 22 (5), 1980, 1916–1929.

[14]. Froese Fischer C, Breit-Pauli lifetimes and transition probabilities for SiI, Phys. Rev. A, 71, 2005, 042506.
[15]. Smirnov Yu M, Excitation of gallium one-charged ion in e-Ga collisions, J. Phys. B: At. Mol. Opt. Phys. 48 (16), 2015, 165204 (11pp.).
[16]. Smirnov Yu M, TlII excitation cross-sections in collisions of slow electrons with thallium atoms, J. Phys. B: At. Mol. Opt. Phys. 49 (17), 2016, 175204 (11pp.).
[17]. Martin W C and Zalubas R, Energy levels of silicon, J. Phys. Chem. Ref. Data, 12 (2), 1983, 323–380.

*Smirnov Yu.M.. "Excitation Of Silicon Atom And Singly-Charged Ion In E–Si Collisions" International Journal of Research in Engineering and Science (IJRES), vol. 06, no. 01, 2018, pp. 70–78